www.rericjournal.ait.ac.th

Integration of Renewable Energy Distributed Generation and Battery Energy Storage in Radial Power Distribution System

Elifuraha Reuben Mmary*,[1] and Boonruang Marungsri[+]

Abstract – *In the modern world power system generation, transmission, distribution and its efficient usage defines the development of the country. In distribution system of an electrical network due to the influence of increased load demand, fluctuation of voltage profile and high power losses are to be focused indeed. To avoid these technical problems in power distribution network, renewable energy distributed generation (REDG) plays a vital role in the radial distribution system. However,hybrid optimization technique which combines artificial bee colony (ABC) and Cuckoo Search (ABC/CS) algorithm are recently techniques employed to solve multi-objective problems by considering both voltage magnitude and power factor constraints. The location found by voltage stability index (VSI) which validated by ABC and sizing of REDGs found by ABC/CSA. The analysis of the present research paper guide to installation of REDGs which lead to simultaneously reduction of both active and reactive power as multi-objective functions. Simulated results such as power losses of the system and cost of REDG, cost of energy losses validated in IEEE 33-nodes and 69-nodes systems and compared with other optimization techniques reviewed in the literature.*

Keywords – *Artificial bee algorithm, CSA, hybrid ABC/CS, renewable energy DG, VSI.*

1. INTRODUCTION

Electric power distribution systems are in a continuous state of evolution into a smart system. The massive penetration of REDG and energy storage into power distribution grid are the salient features of the smart grid. However, the integration of REDGs perturbs the power flow, energy loss, investment cost and cost of energy (COE) of the network [1]. So, voltage stability and energy loss in power distribution network are the significant issues to be addressed. Some of the solutions proposed by different researchers are integration of REDGs, network reconfiguration, feeder restructuring, and placement of capacitor into the radial distribution network.

The optimal integration of renewable energy DG (REDG) in distribution network are the important power source that helps to enhance performance. Since, the optimal location, number, type of technology and size of REDG are the good option for improving voltage stability, reduce power loss, network congestion and power quality [2]. Wind turbine based on PMSG and Solar PV type take the prominent position among all other sources due to its continuous availability, supplying of reactive and cost-effectiveness of the operation in the distribution network. The benefits of integration hybrid REDG units in distribution systems provide significant savings in the cost of energy losses, and performance enhancement of PDG [3] as compared to network reconfiguration and feeder restructuring. Wind energy and solar PV are the fastest growing sources of energy to the market now a days. Henceforth, to take more benefits, REDGs should be merged optimally so that system operations can improve with the integration of multiple REDGs [4].

Numerous optimization methods have been suggested in the literature for optimal placement and capacity of REDGs [5]–[6]. But, due to nature of the problem in power distribution network, the classical optimization techniques require large computation capacities for the solution of the large network [6]. Currently, there are many metaheuristic algorithms oriented to the optimization and solution of an engineering problem. These algorithms include Particle swarm optimization (PSO) [5], [7], the Genetic algorithm (GA) [8], Cuckoo Search Algorithm [9], BAT Algorithm [10], IWO [17] and analytical expression based heuristics [11]. However, the limitation of analytical expression based heuristics inability to handle multiobjective and multiple REDG.

The optimal selecting of REDG has been investigated in the radial distribution system to minimize power losses through analyzing different types of REDG. The REDG which is capable of injecting both active and reactive power is the most effective for power loss reduction. However, many authors investigated actual power loss by considering the integration of multiple REDGs [12]–[14] with only one objective function. Multiobjective optimization problem (MOOP) has been solving by either a single objective optimization using weight factor approach or handing multiple objective optimization problems simultaneously [15]–[16].

Most of the presented research studies [17]–[19] have assumed that REDG operates at unity power factor. It is found that only the location and size have been considered, while the optimal power factor for each REDG is a crucial part of minimizing energy losses. However, some of the authors [20] solved the optimal placement problem of REDG by the analytical approach,

*Dar es Salaam Institute of Technology, Dar es Salaam, Tanzania.

[+]School of Electrical Engineering, Suranaree University of Technology, Thailand.

[1] Corresponding author;
Tel: + 66 611294190.
E-mail: reubsonmmary@gmail.com.

evolutionary computing, and intelligent techniques. Only the real power output of REDGs was considered in these approaches. The main contribution of this paper is to propose the hybrid ABC/CS algorithm to optimally locate multiple REDG by considering multiobjective optimization of REDG with node voltage constraints. Despite constraints, both real and reactive power losses reduction were considered at 0.9 pf compared to unit pf found in the literature. Batteries energy storage used to overcome the intermittent nature of REDG [21]. According to the potential of renewable energy source and the purpose of using a hybrid system, different configurations presented which include WT, solar PV and energy storage systems.

Apart from different AI algorithms such as PSO [5], DE [4] and IWO [15], there is a need of increase flexibility and capacity by combining two techniques for a better solution of optimizing PDG. It acknowledged that the CSA and ABC are the recently meta-heuristic algorithms tested to solve the optimization problem in engineering. However, the hybrid ABC/CSA demonstrates high competence and outperforms other methods regarding fast convergence, accuracy, and simplicity in concept and ease of implementation. It generates new solution considering previous selected solution in a vector and offering the flexibility of the better solution. The rest of the paper is organized as follows: Section 2, describes the modeling of REDG. Section 3, details about problem formulation. Section 4, introduces a methodology for integrating REDG into radial distribution networks. Section 5, describes numerical results and discussions of 33 nodes and 69-node test distribution system. Finally, Section 6 summaries the contributions of this research work.

2. MODELING OF REDG UNITS

2.1 The Grid-connected Hybrid REDGs Units

In Figure 1 below depicts the components of the proposed hybrid system which comprises solar PV, wind turbine based on PMSG, and battery energy storage as REDG.

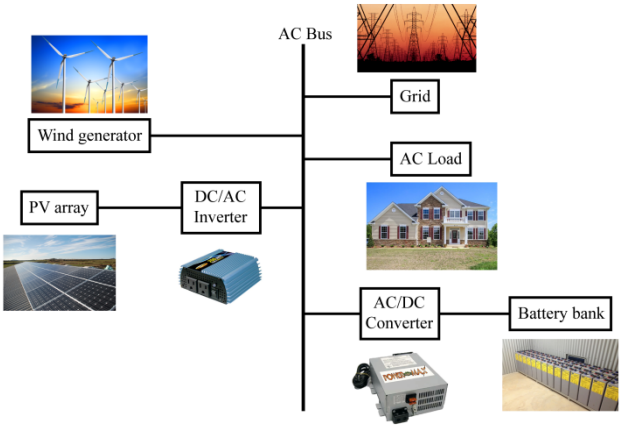

Fig. 1. Grid-connected hybrid REDG.

2.2 Wind Turbine

The modeling of RES is a significantly important part of the analysis. The impacts of integrating REDG on distribution system parameters have to be studied before integration in order to ensure system security and reliability. For calculation of power output in wind turbine, two main factors must be known: the wind speed on a particular location and the power curve of the wind turbine. According to [22] the power curve of a wind turbine can be modeled using a function split into different parts as shown in Equation 1.

In this paper, model type of wind turbine used available in [20]. The parameters of PMSG based wind turbine used to model the power curve are as follows: P_{nom}=600 kW, V_{ci}=4m/s, V_{nom}=16 m/s V_{co}=20 m/s. Data in Table 1 shows the average wind speed used to calculate the power generated by the wind turbine generator in the deterministic optimal power flow algorithm.

$$\begin{cases} P_W(v)=\begin{cases} 0 & V<V_{Ci} \\ YP_{norm} & V_{Ci}<V<V_{norm} \\ 0 & V>V_{Co} \end{cases} \\ Y = \dfrac{V^2-V_{Ci}^2}{V_{norm}^2-V_{Ci}^2} \end{cases} \quad (1)$$

Where P_{nom}, V_{nom}, V_{ci}, *and* V_{co} *are* nominal power, wind speed, cut-in wind speed, and cut-out wind speed of the wind turbine, respectively. P_w is the electric power output of the wind turbine, *V is the* speed of the wind turbine.

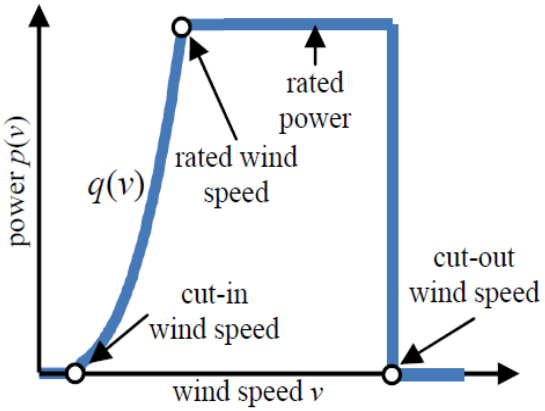

Fig 2. The power curve of the wind turbine.

The expression given in Equation 2 used to represent the non-linear part of the power curve q(v) from Figure 2 above.

$$q(v)=0.5\rho AC_p V^3 \quad (2)$$

The equation given in Equation 3 demostrates the relationship between the rated power and rated wind speed.

$$P_r(v)=0.5\rho AC_p V_r^3 \quad (3)$$

Where;

ρ Air density in kg/m^3

A Swept area of the rotor in m^2
C_p Power coefficient
V_r Rated wind speed value in m/s^2
P_r Rated power of WT

For SCIG, the amount of consumed reactive power is uncontrolled because it varies with wind conditions. However, the reactive power supplied with a grid to a wind turbine (SCIG) causes additional power losses into transmission and distribution which may cause instability of the system and even transient during switching-in. PMSG is preferred because of drawbacks of SCIG such as voltage instability in case fault without compensation of reactive power. When the fault cleared, SCIG draws a significant amount of reactive power. Figure 3 shows output characteristics connected to the grid which may lead to further voltage variations.

The output characteristics of squirrel-cage induction generator (SCIG) shown in Figure 3 detail the information which may lead to further voltage variation in the on-grid system. In this research paper, a hybrid of PMSG, solar PV and BES used to mitigate the problem of reactive in power distribution grid.

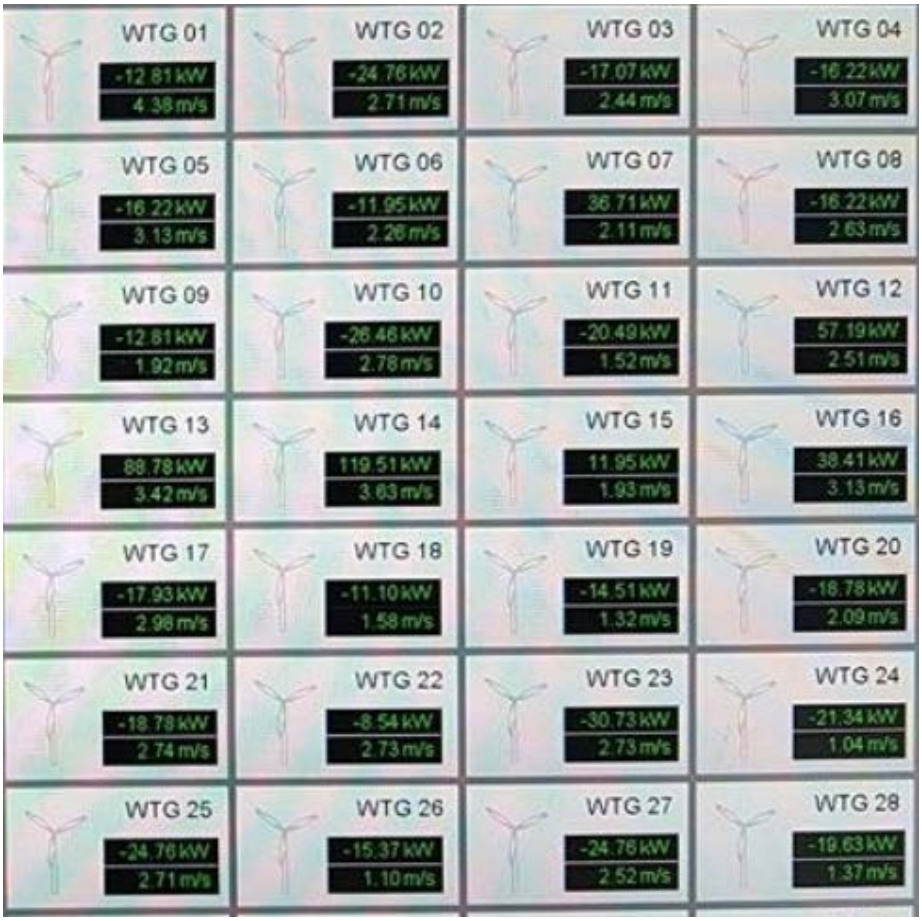

Fig. 3. Output power (in kW) of SCIG-wind turbines.

2.3 Solar PV

The total energy emitted by the sun is $63MW/m^2$. The inverse square law used to determine the solar radiation is striking the earth surface. It means that the total radiant energy striking the earth's surface is inversely proportional to the square of the distance. For double the distance, this energy reduces to a quarter of the original energy. Only about 40% of the solar energy which is intercepted by the earth is passed through the atmosphere and is available for solar applications

The power of the solar PV shown in Equation 4 depends on the technical parameters such as ambient temperature and solar irradiation [14], [22]. The Equations 5 and 6 were used to calculate the power output of the solar PV and average temperature of the cell.

$$P_{PV} = \frac{P_{STC} I_S}{1000}[1+\mu(T_C - 25)] \quad (4)$$

Where;
P_{STC} Maximum power of photovoltaic at standard test condition (STC) in Watts
I_s Solar irradiance on the Solar PV surface (W/m^2),
μ Solar PV temperature coefficient
T_c Photovoltaic cell (module) temperature (°C).

The photovoltaic module temperature in Equation 5 calculated as a function of solar irradiance and ambient temperature based on the module's nominal operating cell temperature (NOCT).

$$T_C = T_a + \frac{I_S}{1000}(T_{NOCT} - 20) \quad (5)$$

Where;

T_a Ambient temperature (°C),
T_{NOCT} Nominal operating temperature of solar PV

Sun module of SW 250 mono modules are used in this paper. Their performance characteristics are:
P_{STC} = 250 W, μ=0045 $^0C^{-1}$, T_{NOCT} = 46 ^{0}C.

During the process of nuclear fusion, the sun produces energy that in the form of electromagnetic waves (radiation). Solar insolation is affected by factors such as atmosphere, the angle of the sun and distance. The thinner the atmosphere in which the sun is passing through, the more the insolation. Insolation is also at its highest when the sun is directly overhead in an area. This is also the shortest distance between the sun and an area. When the angle of the sun to an area increases, the distance increases, and a lot of energy is lost through reflection. Insolation refers to the quantity of solar radiation energy received on a surface area during an amount of time T.

In the photovoltaic industry average irradiance expressed in watt per square meter (W/m²) as depicted in Table 1. For global solar potential, the total solar irradiance upon the earth (TSI) amounts to 1.361 kW/ m², which in theory, on earth with a surface area of about 510,000,000 km^2 yield a total of 694.11TW. Data in Table 1 present the average solar radiation used to determine the power generated by the solar PV generator in the deterministic optimal power flow algorithm.

Table 1. Parameters used in REDG.

S/N	Parameter	Value
1	Power coefficient Cp	0.59
2	Air density ρ (kg/m^3)	1.225
3	Wind generator efficiency	0.85
4	Average wind speed in m/s^2 per year	5.1
5	Average solar radiation (W/m^2)	4.98

3. PROBLEM FORMULATION

Most of the real world problem are associated with the simultaneous optimization of several objective functions. The goal of the proposed method is to minimize active and reactive power losses and hence reduce the cost of energy losses as shown in Equation 6 and subjected to constraints in Equation 7 [24].

$$\min \ [P(x,u), Q(x,u), C_{EL}(x,u)] \tag{6}$$

Subjected to;

$$\begin{cases} g(x,u)=0 \\ h(x,u) \le 0 \end{cases} \tag{7}$$

Where;
P is the multi-objective function comprise of power loss, cost of energy and reactive power loss.
g is the equality constraints
h is the inequality constraints
x and *u* are vectors of state and control variables, respectively.

The vector of state variables *x* expressed in Equation 8 as follows:

$$x = [P_{Slack}, V_L, S_l, Q_G]^T \tag{8}$$

Where;
V_L Voltage of load nodes
S_l Thermal limits of the line.
Q_G Generated Reactive power
P_{slack} Slack power at the slack bus

The vector of control variables *u* expressed in Equation 9 as follows:

$$u = [V_{PV}, P_{DG},]^T \tag{9}$$

Where;
V_{PV} Voltage at PV nodes
P_{DG} Power generated from renewable DG
T Tap setting of the transformer

3.1 Multi-Objective Functions

Formulated multiobjective problem converted to single objective optimization problem by a linear combination of three objective functions. These functions are active power loss, reactive power loss and cost of energy loss illustrated in Equations 10, 11, and 12, respectively.

3.1.1 The Total Active Power Losses

$$P=\sum_{k=1}^{N} G_k[V_i^2+V_j^2-2|V_i||V_j|\cos(\delta_i-\delta_j)] \tag{10}$$

Where;
N depicts branches in the system;
Gk conductance of the line 'k,'
V_i and V_j are the magnitudes of voltages of tie line;
δ_i and δ_j are angles of the end voltages.

3.1.2 The Total Reactive Power Losses

$$Q=\sum_{k=1}^{N} B_k[V_i^2+V_j^2-2|V_i||V_j|\sin(\delta_i-\delta_j)] \tag{11}$$

The optimal sitting of REDG with appropriate size will reduce power losses and cost in the distribution grid.

3.1.3 Cost of Total Energy Losses

The Equation 12 which illustrate cost of energy loss referred from [29].

$$\begin{cases} C_{EL}(\$) = (P_{Loss})(K_p+K_e*Lsf*8760) \\ Lsf=(k_c)(\text{Load factor})+(1-k_c)(\text{load factor})^2 \end{cases} \tag{12}$$

Where;
C_{EL} Cost of energy loss in $
P_{loss} Total Power loss in kW
K_p Annual demand cost of power loss ($/kW)
K_e Annual cost of energy loss ($/kWh)
L_{sf} Loss factor

The value taken for calculation are referred from [28]:
kc = 0.2; load factor = 0.47; K_p = 57.69$/kW, K_e = 0.0096$/kWh.

3.2 System Constraints of the Networks

The full set of system constraints may be written in the standard format $Ax \le b$ where A the matrix and b the vector result from the distribution grid and REDG conditions.

3.2.1 Equality Constraints

The equality constraints shown in Equation 13 represent ideal power balance and power flow equations. However, the power balance equation in a distribution network with REDG units expressed as follows:

3.2.2 Power Flow Equation Limits

The equality function constraints (13) present the power flow equations;

$$\begin{cases} P_S + P_{REDG} - P_D = \sum_{k=1}^{N} G_k[V_i^2 + V_j^2 - 2|V_i||V_j|\cos(\delta_i - \delta_j)] \\ Q_S + Q_{REDG} - Q_D = \sum_{k=1}^{N} B_k[V_i^2 + V_j^2 - 2|V_i||V_j|\sin(\delta_i - \delta_j)] \end{cases} \quad (13)$$

Where;
P_s and Q_s are power purchased from the substation.

3.2.3 Inequality Constraints

Inequality constraints of the system in Equations 14 to 18 are the functional operating constraints containing voltage of generator, reactive power, voltage of load nodes, power factor and penetration level of REDG. However, these constraints may define the feasibility region of the state and control variables

3.2.4 Generator Output Limits

Voltage of generator shown in Equation 14 and reactive power of i^{th} node lie between their upper and lower limits defined in Equation 5 are given as follows:

$$V_{Gi}^{min} \le V_{Gi} \le V_{Gi}^{max} \quad (14)$$

$$Q_{Gi}^{min} \le Q_{Gi} \le Q_{Gi}^{max} \quad (15)$$

Where in Equation 14 depicts minimum and a maximum voltage of i^{th} generating units and in Equation 15 present minimum and maximum reactive power of i^{th} generating units. Equation 16 depicts the minimum and maximum voltage of i^{th} node.

3.2.5 Load Node Constraints

$$V_{Li}^{min} \le V_{Li} \le V_{Li}^{max} \quad (16)$$

3.2.6 Power Factor Constraints

$$pf_{min} \le pf \le pf_{max} \quad (17)$$

3.2.7 Penetration of REDG

$$0 \le S_{REDG} \le S_{Load}^{max} \quad (18)$$

In this research work, Inequality constraints of the dependent variables are load nodes voltage magnitudes and reactive power of REDG units. The new expanded objective function becomes:

$$\begin{cases} F_P = F + \lambda_V \sum_{i=1}^{NL} (V_i - 1)^2 + \lambda Q_{DG} \sum_{i=1}^{NPV} (Q_{DGi} - Q_{DGi}^{lim})^2 \\ + \lambda_S \sum_{i=1}^{N} (S - S_i^{lim})^2 \end{cases} \quad (19)$$

Where;
λV, λ_{QDG}, and λ_S are defined as penalty factors.

3.3 Voltage Stability Index (VSI)

The voltage stability index (VSI) shown in Equation 20 calculated for all of the nodes, since the nodes with max voltage stability index near to 1 are prone to voltage instability, and it is essential to distinguish weak nodes. A node with VSI near to zero is more stable than other above 0.5. Also, results of VSI using Equation 18 were compared with VSI from [29].

$$VSI = \frac{4X}{V_i^2}\left(\frac{P_j^2}{Q_j} + Q_2\right) \le 1 \quad (20)$$

Table 2. Limits of control variable.

Variable	Limits
Generator voltage	0.95 - 1.05
P_{RDG}(MW)	1.5 - 4

4. METHODOLOGY

4.1 Artificial Bee Colony (ABC)

Currently, a new intelligent search algorithm called ABC which mimics the natural behavior of honey bee in searching food sources is adapted in this research article. It is an efficient method introduced by Karaboga in 2005 with parameters shown in Table 3 for solving optimization problems [19].

4.2 An Optimization Algorithm for ABC

Step 1: Initialize the food-source locations X_i (solutions population), The X_i form is as follows:

$$X_{ij} = X_{min} + rand(0.1)(X_{max,j} - X_{min,j} \quad (21)$$

Step 2: Calculate the nectar amount of the population using their fitness values using:

$$Fitness = \frac{1}{1 + objective\_function} \quad (22)$$

Total Losses= objective function = P_Loss + Q_ Loss
Step 3: Produce neighbor solutions for the employed bees by using Equation 23.

$$V_{ij}=X_{ij}+f_{ij}(X_{ij}-X_{kj}) \quad (23)$$

Step 4: Apply the acquisitive selection process between Xij and Vij. If all onlooker bees distributed, go to *Step* 8. Otherwise, go to next step.

Step 5: Determine the probability values $P(X_{ij})$ for the solutions X_{ij} using Equation 24.

$$P(X_{ij}) = \frac{F(X_i)}{\sum_{i=1}^{N} F(X_i)} \quad (24)$$

Step 6: Produce the new solutions *Vi* for the onlookers from the solutions xi, depending on Pi apply the greedy selection process between X_{ij} and V_{ij}.

Step 7: Determine the abandoned solution for the scout bees, if it exists, and replace it with an entirely new solution using equation and evaluate them as indicated in Step 2.

$$X_{i,j}^{new}=X_{min,j}+rand(0,1)(X_{max,j}-X_{min,j}) \quad (25)$$

Step 8: If cycle = MCN, stop and print result.

Table 3. Parameters of ABC in IEE 34 system.

S/N	Parameters	Value
1	Population	20
2	Generation	80
3	Scaling factor	0.9
4	Crossover rate	0.5
5	Decision variable	14

Table 4. Weight factor used for simulation.

Cases	Kp	Kq	Ke
1	1	0	0
2	0.5	0.5	0
3	0.4	0.3	0.3

From Table 4, the summation of weight factor (K_p, K_q, and K_e) should be equal to one.

4.3 Proposed Hybrid ABC/CS Algorithm

The structure of proposed method utilizes a hybrid ABC and CSA. The objectives considered in proposed framework minimize power losses and the cost of energy losses. Based on multiobjective function VSI and ABC employed for optimal allocation of REDG with suitable size obtained by ABC/CSA. The algorithm of suggested method is shown in Figure 4. While convergence of the proposed method is shown in Figure 5.

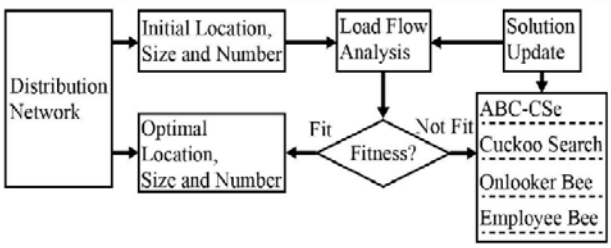

Fig. 4. The proposed architecture of ABC/CSA.

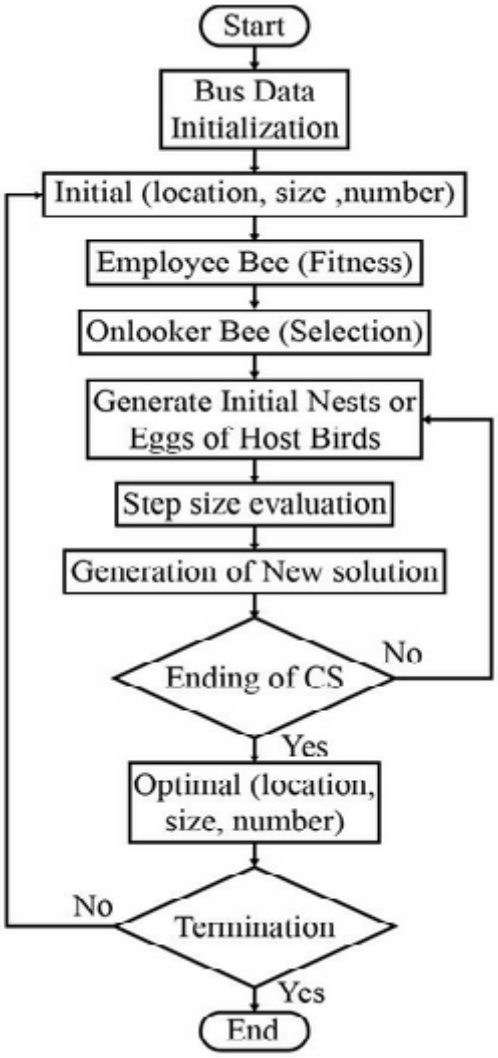

Fig. 5. Scheme of optimizing REDG using ABC/CSA.

The simulation results shown in Figure 6 are the outcomes of utilizing control variables in Table 2 and weight factors in case 3 from Table 4.

5. SIMULATION RESULT AND DISCUSSION

The effectiveness of ABC/CSA tested on IEEE 33-nodes and IEEE-69-nodes systems [26]-[27].

5.1 Results for 33-Nodes Test System using ABC/CSA with VSI at Case # 3

In Figure 7, it shows a line diagram of the 12.7kV, 33-nodes radial distribution system. It has one feeder with four different laterals, 32 branches and a total peak load of 3715kW and 2300kVAr. The total power loss of the system at the base case system is 221.20kW and 143.7kVAr before installation of REDG into the system. With installation of REDG at unity power factor, real and reactive power losses were 107.5kW and 64.1kVAr respectively. Penetration of REDG at 0.9 pf real and reactive power losses become 54.18kW and 32.59kVAr respectively with REDGs at nodes 18 and 33.

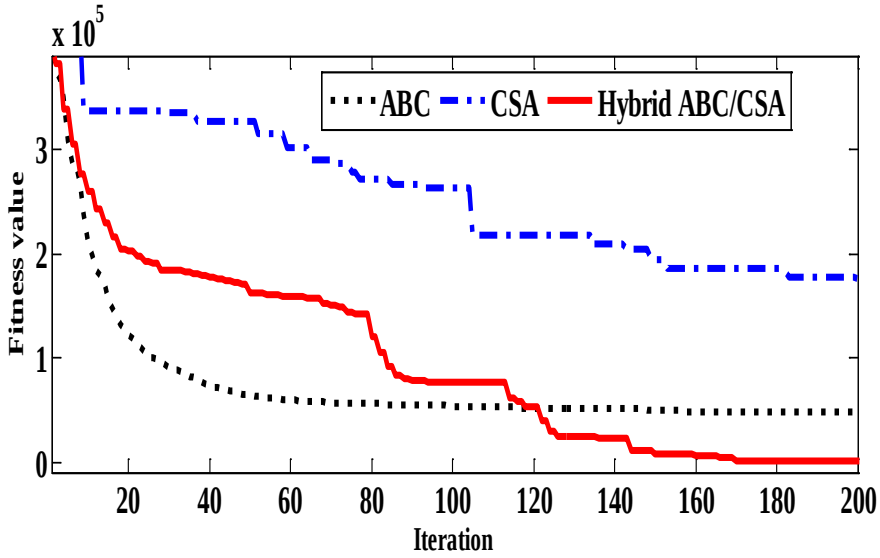

Fig. 6. Convergence characteristics of ABC/CSA.

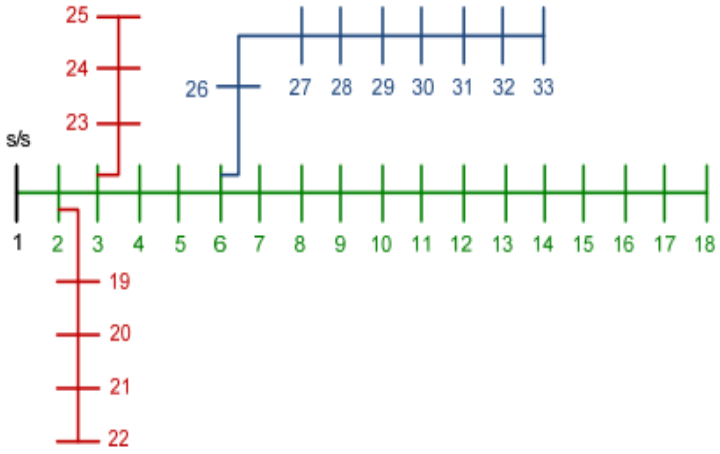

Fig. 7. The 33-nodes test radial distribution system.

Table 5. Results of 33-nodes at a unity power factor.

	Without REDG	SFLA [27]	ABC/CS
REDG Location	-	30	18
REDG size MW	-	1.54	1.25
P loss kW	221.4	125.16	107.5
Q loss kVAr	143.7	98.16	64.1
Vmin	0.91	0.94	0.95
Cost of EL $	19641.4	10067.59	55135.3
Cost of P_{REDG} $/MWh	-	31.10	25.4

Table 6. Results of 33-nodes at 0.9 power factor with REDG.

	SFLA [27]	ABCCS
REDG Location	30	18, 33
REDG size MW	1.74	2.34
P loss kW	78.43	54.18
Q loss kVAr	58.97	32.59
Vmin	0.95	0.97
Cost of EL $	6,308.92	4,105.02
Cost of P_{DG} $/MWh	35.17	41.22
Cost of S_{DG} $/MVA	38.88	46.08

5.2 Results for 69-nodes Test System using ABC/CSA with VSI

Illustration of the single line rated 12.66kV, shown in Figure 8, has 69-nodes test radial distribution system. It has one feeder with eight laterals, 68 branches, a total peak load of 3800kW and 2690kVAr and its corresponding active and reactive power loss are 224.93kW and 102.11kVAr before installation of REDG into the system, respectively. With the installation of REDG at unity power factor, real and reactive power losses were 52.76kW and 37.92kVAr respectively. Penetration of REDG at 0.9 pf real and reactive power losses become 48.11kW and 27.34kVAr, respectively with REDGs at nodes 27 and 65.

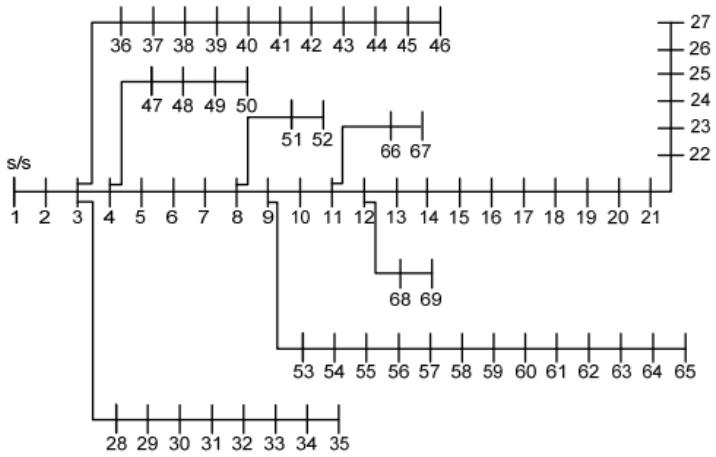

Fig. 8. 69-nodes test radial distribution system.

Table 7. Results of 69-nodes at a unity power factor.

	Without REDG	SFLA [27]	ABC/CS
REDG Location	-	61	22, 65
REDG size MW	-	1.88	1.99
P loss kW	225.56	83.22	52.76
Q loss kVAr	102.11	40.57	37.92
Vmin	0.90	0.96	0.971
Cost of EL $	18,101.70	6,694.3	3,971.2
Cost of P_{REDG} $/MWh	-	37.69	50.68

Table 8. Results of 69-nodes at 0.9 power factor with REDG.

	SFLA [27]	ABC/CS
REDG Location	61	27, 65
REDG size MW	1.57	2.20
P loss kW	57.92	48.11
Q loss kVAr	46.47	27.34
Vmin	0.964	0.977
Cost of EL $	40.16	32.14
Cost of S_{DG} $/MVA	44.44	52.04

5.3 Cost of REDG, Cost of Energy Losses and Saving

Cost of REDG determined by the following formula

$$C(P_{REDG}) = aP_{REDG}^2 + bP_{REDG} + c \quad (26)$$

Where;

a = 0;
b = 20;
c = 0.25

Both a, b and c are the cost coefficient of REDG defined in [29].

Fitness function for maximum saving

$$S = K_P\Delta P + K_E\Delta E - K_{REDG}S_{REDG} \quad (27)$$

Where;

S	Saving in $/year
K_p	Factor of convert power losses to $
K_E	Factor of converting energy losses into $
K_{REDG}	Cost of REDG
S_{REDG}	Capacity of REDG

Tables 5 to 8 shows that both real and reactive power losses in radial distribution get reduced with the

insertion of hybrid REDG in 33-nodes and 69-nodes network. BES utilized at the moment of deficiency power from hybrid REDG. Wind turbine based on PMSG, solar PV and BESS improve the performance of radial distribution system efficiently than DFIG which consume reactive power and supply only active power. Since the primary problems in distribution system are unbalanced of reactive power which leads to voltage variations and high power losses.

6. CONCLUSION

In this paper, ABC/CSA and VSI have been used for sizes and location of REDG in the radial distribution system. Analysis of this paper carried out with unit power factor, and 0.9 pf leading operated REDG. The optimal size of WT based on the permanent magnet synchronous generator and solar PV are used to improve voltage profile through supplying both active and reactive power in the power distribution grid. A performance which gives better results of cost and power loss into distribution network improved with REDG at 0.9 pf. The results support the integration of optimal REDG and BESS in the radial distribution system and thereby make the power system environment friendly.

REFERENCES

[1] Yeh H.G, Gayme D.F, and Low S.H., 2012. Adaptive VAR control for distribution circuits with photovoltaic generators. *IEEE Transactions in Power Systems* 27: 1656–1663,

[2] Kursat A., 2012. Artificial bee colony algorithm solution for optimal reactive power flow. *Applied Soft Computing* 12(5): 1477–1482.

[3] Thomson M., 2007. Network power-flow analysis for high penetration of distributed generation. *IEEE Transactions in Power Systems* 22(3): 1157–1162

[4] Varadarajan M. and K.S. Swarup. 2008. Differential evolutionary algorithm for optimal reactive power dispatch. *Electrical Power and Energy Systems* 30(8): 435–441.

[5] Altaf Q.H, Umre B.S, and Junghare A.S., 2012. Reactive power control using dynamic particle swarm optimization for real power loss minimization. *Electrical Power and Energy Systems* 41(1): 133–136.

[6] Reza S., Azah M., and Hussain S., 2012. Optimal allocation of shunt var compensators in power systems using an ABC algorithm. *Electrical Power and Energy Systems* 43(1): 562–572.

[7] Mounika L., Prasanna K., Jain A., and James R., 2017. Particle Swarm optimization application for optimal location of multiple distributed generators in power distribution network. *Journal of Electrical and Electronic System* 6(4): 244–249.

[8] Moradi M.H. and M. Abedini. 2012. A combination of genetic algorithm and particle swarm optimization for optimal DG location and sizing in distribution systems. *Electrical Power and Energy Systems* 34: 66–74,

[9] El-Fergany A. and A.Y. Abdelaziz. 2014. Efficient heuristic-based approach for multiobjective capacitor allocation in radial distribution networks. *IET Generation, Transmission, Distribution* 8(1): 70–80.

[10] Zeinalzadeh A, Mohammadi Y, and Moradi M.H., 2015. Optimal multi-objective placement and sizing of multiple DGs and shunt capacitor banks simultaneously considering load uncertainty via MOPSO approach. *International Journal of Electrical Power and Energy Systems* 67: 336–349

[11] Shaheen H., Rashed G., and Cheng S., 2011. Optimal location and parameter setting of UPFC for enhancing power system security based on genetic algorithm and differential evolution algorithm. *Electric Power and Energy Systems* 33(1): 94–105.

[12] Mallipeddi R., Jeyadevi S., and Suganthan P., 2012. Efficient constraint handling for optimal reactive power dispatch problems. *Swarm and Evolutionary Computation* 5: 28–36.

[13] Environmental External Costs from Power Generation by Renewable Energies. Available online In http://www.windturbines.ca/vestas_v44.htm. [Accessed on March 20, 2018].

[14] Atwa M. and M.A. Salama. 2011. Adequacy evaluation of distribution system including wind and solar DG during different modes of operation. *IEEE Transaction on Power Systems* 26(4): 1945–1952.

[15] Rama Prabha D. and T. Jayabarathi. 2016. Optimal placement and sizing of multiple distributed generating units in distribution networks by invasive weed optimization algorithm. *Ain Shams Engineering Journal* 7(2): 683–694.

[16] Yang C., Gordon G.L., and Ching-Tzong S., 2012. Optimal setting of reactive compensation devices with an improved voltage stability index for voltage stability enhancement. *Electric Power and Energy Systems* 37(1): 50–57.

[17] Abu-Mouti F.S. and M. El-Hawary. 2011. Optimal distributed generation allocation and sizing in distribution systems via artificial bee colony algorithm. *IEEE Transactions on Power Delivery* 26: 2090–2101.

[18] Mmary E.R. and B. Marungsri. 2018. Multiobjective optimization of renewable distributed generations in radial distribution networks with optimal power factor. *International Review of Electrical Engineering (IREE)* 13(4): 297–304. DOI: https://doi.org/10.15866/iree.v13i4.15069.

[19] El-Fergany A., 2015. Optimal allocation of multi-type distributed generators using backtracking search optimization algorithm. *International Journal of Electrical Power and Energy Systems* 64: 1197–1205.

[20] El-Fergany A., 2014. Involvement of cost savings and voltage stability indices in optimal capacitor allocation in radial distribution networks using artificial bee colony algorithm. *International Journal of Electrical Power and Energy Systems* 62: 608–616.

[21] Murthy V. and A. Kumar. 2013. Comparison of optimal DG allocation methods in radial distribution systems based on sensitivity approaches. *International Journal of Electrical Power and Energy Systems* 53: 450–467.

[22] Abbas R., Maziar V., and Mostafa P., 2012. Optimal reactive power dispatch for improving voltage stability margin using a local voltage stability index. *Energy Conversion and Management* 59: 66–73,

[23] Sajjadi S.M., Haghifam M.-R., and Salehi J., 2013. Simultaneous placement of distributed generation and capacitors in distribution networks considering voltage stability index. *International Journal of Electrical Power and Energy Systems* 46 366–375.

[24] Khodabakhshian A. and M.H. Andishgar. 2016. Simultaneous placement and sizing of DGs and shunt capacitors in distribution systems by using IMDE algorithm. *International Journal of Electrical Power and Energy Systems* 82: 599–607.

[25] Mallanchettiar J. and V. Subathra. 2017. Minimization of cost by simultaneous placement of multi-DGs and capacitors in distribution system using hybrid optimization. *International Journal of Advances in Computer and Electronics Engineering* 2(6): 8–14

[26] Suresh M.V. and E. Belwin. 2017. Optimal placement of distributed generation in the distribution system by using shuffled frog leaping algorithm. *Journal of Engineering and Applied Sciences* 12: 863–868

[27] Karaboga D. and B. Basturk. 2007. A powerful and efficient algorithm for numerical function optimization: artificial bee colony (ABC) algorithm. *Journal of Global Optimization* 39: 459–471

[28] Sooraj K. and A. Kumar. 2016. Energy savings in radial distribution systems with intermittent wind power and probabilistic load demands. *Energy Procedia* 90: 137–144.

[29] Mmary E.R. and B. Marungsri. 2018, Multiobjective optimization of renewable distributed generation and shunt capacitor for techno-economic analysis using hybrid invasive weeds optimization. *GMSARN International Journal* 12: 24–33.